ORIGINAL RESEARCH

Strain Analysis in Patients at High-Risk for COPD Using Four-Dimensional Dynamic-Ventilation CT

Yanyan Xu [1], Tian Liang[2], Yanhui Ma[2], Sheng Xie[1], Hongliang Sun [2], Lei Wang[3], Yinghao Xu[4]

[1]Department of Radiology, Peking University China-Japan Friendship School of Clinical Medicine, Beijing, People's Republic of China; [2]Department of Radiology, China-Japan Friendship Hospital, Beijing, People's Republic of China; [3]Beijing MicroVec. Inc., Beijing, People's Republic of China; [4]Canon Medical Systems, Beijing, People's Republic of China

Correspondence: Sheng Xie, Department of Radiology, Peking University China-Japan Friendship School of Clinical Medicine, Yinghua Street 2#, Chaoyang District, Beijing, People's Republic of China, Tel +86 108-420-5855, Fax +86 1064222963, Email xs_mri@126.com

Purpose: To quantitatively identify abnormal lung motion in chronic obstructive pulmonary disease (COPD) using strain analysis, and further clarify the potential differences of deformation in COPD with different severity of airflow limitation.

Materials and Methods: Totally, 53 patients at high-risk for COPD were enrolled in this study. All CT examinations were performed on a 320-row MDCT scanner, and strain measurement based on dynamic-ventilation CT data was performed with a computational fluid dynamics analysis software (Micro Vec V3.6.2). The strain-related parameters derived from the whole expiration phase ($PS_{max-all}$, $PS_{mean-all}$, $Speed_{max-all}$), the first 2s of expiration phase (PS_{max2s}, PS_{mean2s}, $Speed_{max2s}$) were divided respectively by the changes in lung volume to adjust for the degree of expiration. Spearman rank correlation analysis was used to evaluate associations between the strain-related parameters and various spirometric parameters. Comparisons of the strain-related parameters between COPD and non-COPD patients, between GOLD I (mild airflow restriction) and GOLD II–IV (moderate to severe airflow restriction) were made using the Mann–Whitney U-test. Receiver-operating characteristic (ROC) analysis was performed to evaluate the diagnostic performance of the strain-related parameters for COPD. $P < 0.05$ was considered statistically significant.

Results: Strain-related parameters demonstrated positive correlations with spirometric parameters (ρ=0.275~0.687, $P<0.05$), suggesting that heterogeneity in lung motion was related to abnormal spirometric results. Strain-related parameters can quantitatively distinguish COPD from non-COPD patients with moderate diagnostic significance with the AUC values ranged from 0.821 to 0.894. Furthermore, parameters of the whole expiration phase ($PS_{max-all}$, $Speed_{max-all}$) demonstrated significant differences (P=0.005; P=0.04) between COPD patients with mild and moderate to severe airflow limitation.

Conclusion: Strain-related parameters derived from dynamic-ventilation CT data covering the whole lung associated with lung function changes in COPD, reflecting the severity of airflow limitation in some degree, even though its utility in severe COPD patients remains to be investigated.

Keywords: strain analysis, dynamic-ventilation CT, chronic obstructive pulmonary disease, computed tomography, CT, airflow limitation

Introduction

Chronic obstructive pulmonary disease (COPD) is characterized as nonreversible airflow limitation abnormality, which is currently diagnosed based on spirometric results and respiratory symptoms.[1,2] Nevertheless, there are several limitations for the evaluation of lung ventilatory function with spirometry. First, spirometric results reflect a global changes of lung function without regional information.[3] In other words, it is hard to discriminate the different patterns of underlying pathologic abnormalities, including emphysema, bronchial inflammation, and small airway disease, as well as their distribution in lung.[4–6] Second, spirometric results did not significantly reflect the morphological disorders (eg, emphysema and air trapping) observed on CT images.[7–12] Additional limitation of spirometry is related to the infective risk under current new coronavirus pandemic. As we all know, it is difficult to carry out spirometry without close contact with potential infected patients.

CT can provide in vivo anatomical information to assess the severity of COPD and make up for the limitations aforementioned to some degree. More recently, quantitative CT analysis have been used for monitoring the progression of diseases such as emphysema and air trapping over time in large longitudinal studies (eg, COPDGene, SPIROMICS, MESA).[13–15] Strain analysis based on 4D dynamic-ventilation CT has emerged as a new quantitative measurement to record lung deformation during ventilation, opening a new era for monitoring pathophysiological changes in COPD.[16–18] Mathematically speaking, strain on a point of a deformable body is determined from the derivatives of the displacement field that deforms the body.[19–23] Xu et al[17] have firstly introduced strain analysis in COPD to monitor pulmonary motion during ventilation. Although that study demonstrated the potential of strain measurement for evaluating pulmonary mechanics, only the "middle" field of the lung were analyzed with single strain-related parameter (maximum principal strain).[17] Despite the significant correlations were observed between the strain-related parameter and spirometry, evidence that strain measurement can reflect lung function changes was insufficiently presented. Considering the regional heterogeneity of emphysema in COPD, especially in the upper-lower direction,[3–5] substantial improvements in the method of strain analysis, particularly analyze scope covering the whole lung and multi-dimensional parameters setting, are needed.

Consequently, the strain analysis performed by a computational fluid dynamic analysis software covering the whole lung was introduced to monitor lung motion during ventilation. The purpose of our study was to quantitatively identify abnormal lung motion in patients at high-risk for COPD, and further clarify the potential differences of deformation in COPD with different severity of airflow limitation. In addition, we also intended to explore the possibility of monitoring lung function using strain analysis in the future.

Materials and Methods

The retrospective study protocol complied with the Declaration of Helsinki for medical studies, and it was approved by the Institutional Review Board at China-Japan Friendship Hospital (approval No. 2020–53-K31), and all participants provided written informed consent.

Subjects

Totally, 70 subjects at high-risk for COPD were recruited in this study between August 2020 and June 2021. The inclusion criteria were: 1) ≥18 years old; 2) ex-/current smoking or long-term (at least one year) passive smoke exposure accompanied with respiratory symptoms (eg, cough, sputum production, or dyspnea); 3) no acute respiratory infection or other severe pulmonary distortion such as interstitial lung diseases or tuberculosis that could affect the quantitative CT measurement; 4) no previous thoracic operation; 5) the interval between CT examinations and spirometry within 2 weeks.

However, subjects who met any of the following criteria were excluded from the late analysis: 1) poor cooperation with voice guidance during dynamic-ventilation CT (n=11); 2) poor image quality that unable to carry out strain analysis (n=3); 3) measurement items of spirometry were incomplete (n=3). Finally, 53 subjects (36 men and 17 women; mean age, 57.87 years; age range, 30–85 years) were enrolled in the study. Detailed clinical characteristics of the subjects enrolled in were summarized in Table 1.

CT Scans Protocol

All patients underwent both conventional low-dose chest CT and dynamic-ventilation CT scans on a 320-row MDCT scanner (Aquilion *ONE*, Canon Medical Systems, Japan). Subjects underwent conventional low-dose chest CT at full inspiration in the supine position.

Parameters for the conventional low-dose chest CT were as follows: tube currents = automatic exposure control (AEC); tube voltage =120 kVp; scanning method = helical scanning; rotation time =0.35 s; beam pitch =0.828; imaging FOV =320 mm; collimation = 0.5 mm ×80 rows; slice thickness =1 mm; reconstruction kernel = FC17 (for mediastinum); iterative reconstruction = adaptive iterative dose reduction using three-dimensional processing (AIDR3D; mild setting); slice thickness/interval=0.5mm/0.5mm.

All participants were coached on continuous deep breathing before dynamic-ventilation CT scans. Dynamic-ventilation CT was performed using dynamic volume scan mode (Z_{max}=16cm) without bed movement. Two volumes of

Table 1 Basic Clinical Characteristics and Imaging Measurements of Study Groups

Parameters		COPD (n=35)	Non-COPD (n=18)	$t/z/\chi^2$	*P*
Demographics					
Age (y)		60.66±11.46	55.39±9.74	−1.664	NS
No. of Male		27(77.14%)	9(50%)	4.020	0.045
No. of Ex-/current smoker		24(68.57%)	4(22.22%)	10.247	0.001
BMI		23.62±2.97	26.51±3.90	3.009	0.004
Spirometry					
FVC (L)		3.45±1.10	3.57±1.13	0.364	NS
FEV_1 (L)		2.23±0.89	2.88±0.94	2.449	0.018
FEV_1/FVC*		65.78±9.85	80.57±4.50	−5.597	<0.001
PEF (L)		6.60±2.45	8.25±1.99	2.465	0.017
MMEF75% (L/S)		4.11±2.24	7.10±2.16	4.662	<0.001
MMEF50% (L/S)		1.74±0.96	3.65±1.40	5.842	<0.001
MMEF25% (L/S)		0.48±0.26	1.08±0.56	−4.077	<0.001
MMEF25-75% (L/S)		1.26±0.71	2.81±1.21	−4.508	<0.001
Imaging measurements					
Static CT	LD index (%)*	7.50±13.90	5.30±15.55	−1.146	NS
	TLV (mL)	4710.80±1036.03	3499.11±1498.99	−2.892	0.004
Dynamic-ventilation CT	$PS_{max-all}$*	150.57±168.39	626.00±584.17	−4.658	<0.001
	$PS_{mean-all}$*	14.02±23.98	65.93±106.48	−4.320	<0.001
	$Speed_{max-all}$*	18.30±18.78	49.87±37.53	−4.104	<0.001
	PS_{max2s}*	62.22±76.96	205.34±131.47	−3.794	<0.001
	PS_{mean2s}*	6.25±9.23	18.52±42.12	−4.432	<0.001
	$Speed_{max2s}$*	14.10±14.05	45.05±38.29	−4.157	<0.001

Notes: *Data are expressed as medians ± interquartile range. Except where indicated, data are means ± standard deviation. Strain-related parameters of the whole expiration phase: $PS_{max-all}$, $PS_{mean-all}$, $Speed_{max-all}$. Strain-related parameters of the first 2s of expiration phase: PS_{max2s}, PS_{mean2s}, $Speed_{max2s}$.
Abbreviations: COPD, chronic obstructive pulmonary disease; BMI, body mass index; FVC, forced vital capacity; FEV_1, forced expiratory volume at 1 second; PEF, peak expiratory flow; MMEF, maximum mid-expiratory flow; NS, no significant; LD index, low density index, defined as the percent low attenuation (<-950 Hounsfield units) volume of the whole lung; TLV, total lung volume.

dynamic-ventilation CT with 1cm overlap were set to cover the entire thorax. Scanning and reconstruction parameters for dynamic-ventilation CT were as follows: tube current =60 mA; tube voltage =80 kV; rotation time =0.35 s; total scanning time =8.4 s; imaging FOV =320 mm; collimation =0.5 mm; slice thickness =1 mm; reconstruction kernel = FC15 (for mediastinum); reconstruction interval =0.2 s/frame (total 41 frames); iterative reconstruction = AIDR3D (mild setting); slice thickness/interval=0.5mm/0.5mm.

Radiation exposure was calculated using dose-length product (DLP), which was based on CT dose index volumes (CTDIvol). The effective dose (ED) was calculated by multiplying DLP values by a conversion factor of k=0.014mSv•mGy^{-1}•cm^{-1}.[24] For conventional low-dose chest CT, the average DLP was 144.64 mGy•cm and average ED 2.02 mSv. For dynamic-ventilation CT, the average DLP was 521.6 mGy•cm and average ED 7.30 mSv.

Image Analysis – Low Density Index (LD Index), Total Lung Volume (TLV) by Static CT

Using commercially embedded software (Lung density analysis, Canon Medical Systems, Japan), the low attenuation (threshold, <-950 Hounsfield units [HU]) on images was automatically identified, and the percent low attenuation (<-950 Hounsfield units) volume of the whole lung (LD index), as well as TLV, was automatically measured.

Image Analysis – Lung Volume-Time Curve by Dynamic-Ventilation CT

Using the same commercial software (Lung density analysis, Canon Medical Systems, Japan), the lung volume of the scanned lung was automatically measured in each frame, then a lung volume-frame curve (Figure 1) was obtained. On
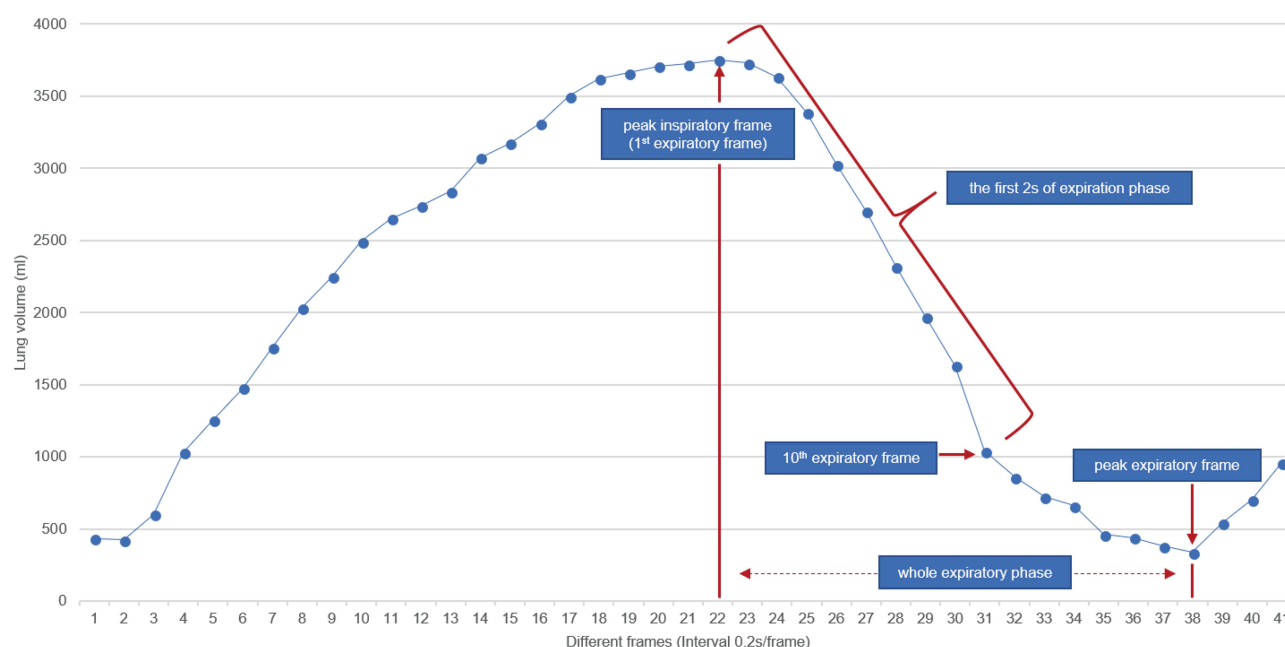
Figure 1 Lung volume-frame curve.

the volume-frame curve, the frame with the maximum lung volume was defined as the peak inspiratory frame (=first expiratory frame), and the expiratory phase defined as the process from the peak inspiratory frame (=first expiratory frame; maximum lung volume frame) to the peak expiratory frame (minimum lung volume frame) on lung volume-frame curve.

Image Analysis – Strain Analysis

Strain analysis was performed on dynamic-ventilation CT using a computational fluid dynamics analysis software (Micro Vec V3.6.2, Micorvec Pte Ltd, Beijing, China) as follows (Figure 2):

1. Image matching and fusion. Using the motion coherence algorithm, the upper and lower volume date were matched and joined together. The overlapped cross sections in the dataset were deleted;
2. Data abstraction. Script codes are used to extract all-frame data of different slices, respectively. The image format is converted from Dicom to Tiff.bmp, and the frequency of data acquisition is 10Hz;
3. The displacement field calculation. All-frame data of the same slice was imported into MicroVec software, and the irrelevant areas that was not included in the calculation were concealed by "Mask" function. Then cross-correlation algorithm was used to calculate the cross-correlation of lung image data and derive the maximum displacement time of those data;
4. The strain-related parameters calculation using Tecplot macro-command. The values of strain-related parameters (maximum Principal Strain [PS_{max}], mean Principal Strain [PS_{mean}] and maximum Displacement Speed [$Speed_{max}$]) were calculated and normalized using the following formula. PS_{max} and PS_{mean} referred to the maximum and average strain in the pixel displacement field (velocity field) based on pixel displacement, respectively. And $Speed_{max}$ was defined as the maximum displacement of pixel in the same velocity field.

$$PS_{max} = \frac{(E_{xx} + E_{yy})}{2} + \sqrt{\left(\frac{E_{xy} + E_{yx}}{2}\right)^2 + \left(\frac{E_{xx} + E_{yy}}{2}\right)^2}$$

where E_{xx} is transverse strain; E_{yy} is longitudinal strain; E_{xy} and E_{yx} are shearing strains.
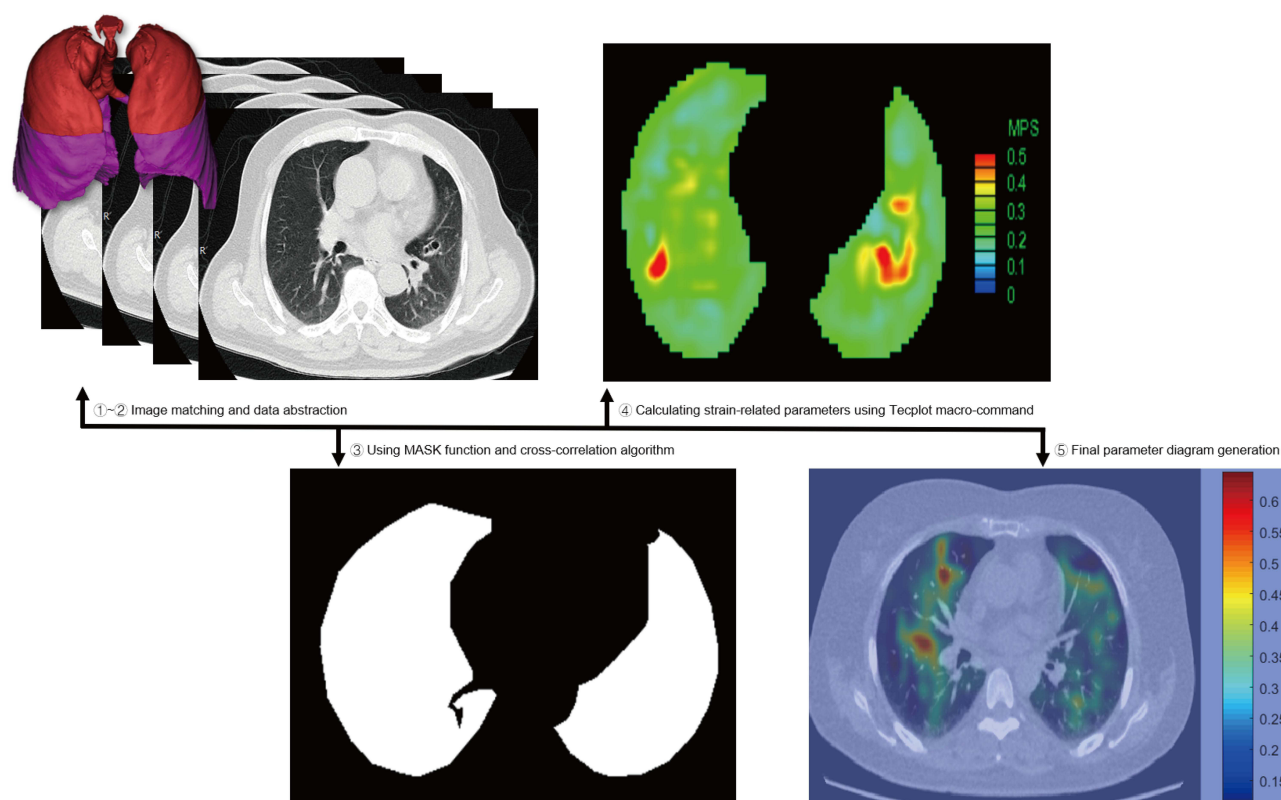
Figure 2 Schematic diagram of strain analysis.

5. The final parameter diagram generation. The pseudo-color fusion image was generated by superimposing the values of different strain-related parameters on the original CT image.

Briefly, in the series of data obtained from dynamic-ventilation CT, only the expiration phase on lung volume-frame curve was included in the analysis. The strain-related parameters (PS_{max}, PS_{mean}, $Speed_{max}$) derived from the whole expiration phase, the first 2s of expiration phase were included in final analysis, respectively. The strain-related parameters' values of the 1st expiratory frame, as well as the lung volume, were selected as the basic reference values. From the 2nd expiration frame, all strain-related parameters' values were divided by the volume changes of corresponding frame to adjust potential influence of expiration degree. Then, adjusted values of all strain-related parameters from 2nd to 10th expiration frame, from 2nd expiration frame to peak expiration frame were summed to express the total strain measurement for different period of expiration phase (PS_{max2s}, PS_{mean2s}, $Speed_{max2s}$; $PS_{max-all}$, $PS_{mean-all}$, $Speed_{max-all}$), respectively.

Spirometry

All subjects underwent spirometry (MasterScreen PFT, Vyaire Medical GmbH, Germany) under the guidance of qualified pulmonary function technicians following the standards published by the American Thoracic Society (ATS) and the European Respiratory Society (ERS).[2] COPD was diagnosed clinically with post-bronchodilator FEV_1/FVC <0.70, and severity was categorized according to Global initiative for Chronic obstructive Lung Disease (GOLD) recommendations.[2] The spirometric parameters included forced vital capacity (FVC), forced expiratory volume at 1 second (FEV_1); PEF, peak expiratory flow (PEF), maximum mid-expiratory flow 75% (MMEF 75%), MMEF50%, MMEF25%, and MMEF25–75%. The interval between spirometry and CT examination was within 2 weeks.

Statistical Analysis

Statistical analysis was performed using SPSS software (SPSS 17.0 for Windows, SPSS, Chicago, IL). The Kolmogorov–Smirnov test for normality was performed on continuous variables and the graphical spread of the data was visually inspected. Descriptive statistics were shown as means ± standard deviation (SD) or medians ± interquartile range (IQR) for continuous variables, and as frequency and percentage for categorical variables. Spearman rank correlation analysis was used to evaluate associations between the adjusted strain measurements and various spirometric values. Comparisons of the strain-related parameters between COPD and non-COPD patients, between GOLD I (mild airflow restriction) and GOLD II–IV (moderate to severe airflow restriction) were made using the Mann–Whitney U-test. Then, receiver-operating characteristic (ROC) analysis was performed to evaluate the diagnostic performance of the adjusted strain parameters for COPD. The areas under the ROC curve (AUC) were calculated: an AUC value < 0.50 indicated poor diagnostic accuracy; an AUC value of 0.51~0.70, fair diagnostic accuracy; an AUC value of 0.71~0.90, moderate diagnostic accuracy; an AUC value > 0.91, high diagnostic accuracy. The cut-off values with the largest Youden index [(sensitivity + specificity) - 1] were calculated from the ROC curves. For all the analyses mentioned above, $P<0.05$ was considered statistically significant.

Results

A total of 53 subjects were enrolled, including 18 non-COPD and 35 COPD patients. The latter group included 19 GOLD I, 12 GOLDII, and 4 GOLD IV. Basic clinical characteristics and imaging measurements of all subjects were summarized in Table 1.

All subjects underwent spirometry and CT scans, including conventional low-dose chest CT and dynamic-ventilation CT. The average interval time between the two kinds of examinations was (7.8±3.4) days.

Correlation Between CT Measurements and Spirometry

The adjusted strain-related parameters, especially the ones derived from the first 2s of expiration (PS_{max2s}, PS_{mean2s}, $Speed_{max2s}$), were significantly correlated with FEV_1/FVC ($\rho=0.450\sim0.687$, $P<0.001$), serial parameters of MMEF ($\rho=0.364\sim0.643$, $P<0.05$), and PEF ($\rho=0.275\sim0.456$, $P<0.05$), suggesting that heterogeneity in lung motion associated with impaired lung function (Table 2).

Table 2 Correlations Between CT Measurements and Spirometry

CT Measurement		Correlation Coefficients (ρ)							
		FVC	**FEV₁**	**FEV₁/FVC**	**PEF**	**MMEF75%**	**MMEF50%**	**MMEF25%**	**MMEF25-75%**
Dynamic-ventilation CT	$PS_{max-all}$	0.121 (NS)	0.237 (NS)	0.450 (P <0.001)	0.251 (NS)	0.396 (P =0.003)	0.397 (P =0.003)	0.420 (P =0.002)	0.410 (P =0.002)
	$PS_{mean-all}$	0.208 (NS)	0.354 (P =0.004)	0.614 (P <0.001)	0.340 (P =0.013)	0.514 (P <0.001)	0.543 (P <0.001)	0.569 (P <0.001)	0.591 (P <0.001)
	$Speed_{max-all}$	−0.026 (NS)	0.187 (NS)	0.679 (P <0.001)	0.262 (NS)	0.436 (P =0.001)	0.438 (P =0.001)	0.364 (P =0.007)	0.467 (P <0.001)
	PS_{max2s}	0.122 (NS)	0.324 (P =0.018)	0.621 (P <0.001)	0.354 (P =0.004)	0.585 (P <0.001)	0.547 (P <0.001)	0.542 (P <0.001)	0.564 (P <0.001)
	PS_{mean2s}	0.264 (NS)	0.431 (P =0.001)	0.652 (P <0.001)	0.456 (P =0.001)	0.616 (P <0.001)	0.612 (P <0.001)	0.597 (P <0.001)	0.643 (P <0.001)
	$Speed_{max2s}$	−0.023 (NS)	0.193 (NS)	0.687 (P <0.001)	0.275 (P =0.046)	0.467 (P <0.001)	0.455 (P =0.001)	0.371 (P =0.006)	0.475 (P <0.001)
Static CT	LD index	−0.094 (NS)	−0.210 (NS)	−0.370 (P =0.006)	−0.047 (NS)	−0.231 (NS)	−0.337 (P =0.013)	−0.338 (P =0.004)	−0.336 (P =0.014)

Notes: Strain-related parameters of the whole expiration phase: $PS_{max-all}$, $PS_{mean-all}$, $Speed_{max-all}$. Strain-related parameters of the first 2s of expiration phase: PS_{max2s}, PS_{mean2s}, $Speed_{max2s}$.
Abbreviations: FVC, forced vital capacity; FEV₁, forced expiratory volume at 1 second; PEF, peak expiratory flow; MMEF, maximum mid-expiratory flow; NS, no significant. LD index, low density index, defined as the percent low attenuation (<-950 Hounsfield units) volume of the whole lung.

Comparison of CT Measurements Between Study Groups

Male, ex- or current smoker, and lower BMI subjects were more frequently observed in COPD group. According to static CT data, TLV in COPD group was significantly larger than that in non-COPD group (P=0.004), whereas the values of spirometric parameters showed the opposite trend, suggesting that more invalid aerated lung tissue may be in COPD patients.

By comparison of COPD group and non-COPD group, all the values of strain-related parameters in COPD group were significantly lower than those in non-COPD group (P<0.001). In addition, compared to GOLD I patients, even though lower values of strain-related parameters were observed in GOLD II–IV, only parameters of the whole expiration phase ($PS_{max-all}$, $Speed_{max-all}$) demonstrated statistically significant difference (z=−2.782, P=0.005; z=−2.053, P=0.04; Table 3).

Predictive Significance of Strain-Related Parameters for COPD

According to the ROC curve, the adjusted strain-related parameters showed moderate diagnostic significance with the AUC values range from 0.821 to 0.894. The PS_{max2s} value for the COPD patients was lower than 65.48 and that for non-COPD patients was greater than 65.48, with the maximal accuracy rate of 86.79% and the maximal sensitivity of 94.29% (Table 4, Figure 3).

Discussion

In this study, strain analysis based on dynamic-ventilation CT data was introduced to quantitatively measure lung deformation during expiration in COPD using a computational fluid dynamics analysis software. Here we reported that strain-related parameters demonstrated positive correlations with spirometric parameters (ρ=0.275~0.687, P<0.05). And strain-related parameters can quantitatively distinguish COPD from non-COPD patients with moderate diagnostic significance. Furthermore, parameters of the whole expiration phase ($PS_{max-all}$, $Speed_{max-all}$) demonstrated significant differences (P=0.005; P=0.04) between COPD patients with mild and moderate to severe airflow limitation. These findings suggest that strain measurements for lung deformation during expiration can reflect lung function impairment to

Table 3 Strain-Related Parameters in COPD Patients with Different Severity of Airflow Restriction

Strain-Related Parameters		GOLD I (n=19)	GOLD II–IV (n=16)	Z	P
Whole expiration	$PS_{max-all}$	186.89±218.86	62.21±118.82	−2.782	0.005
	$PS_{mean-all}$	18.70±27.86	8.17±21.64	−1.788	NS
	$Speed_{max-all}$	21.99±22.66	11.77±20.73	−2.053	0.04
First 2s of expiration	PS_{max2s}	75.58±149.96	52.97±92.92	−1.126	NS
	PS_{mean2s}	7.08±8.22	3.68±15.35	−0.966	NS
	$Speed_{max2s}$	16.58±24.58	10.97±17.56	−1.722	NS

Abbreviations: COPD, chronic obstructive pulmonary disease; GOLD, Global Initiative for Chronic Obstructive Lung Disease; NS, no significant.

Table 4 Cut-off Values and Corresponding Diagnostic Rate for Strain-Related Parameters

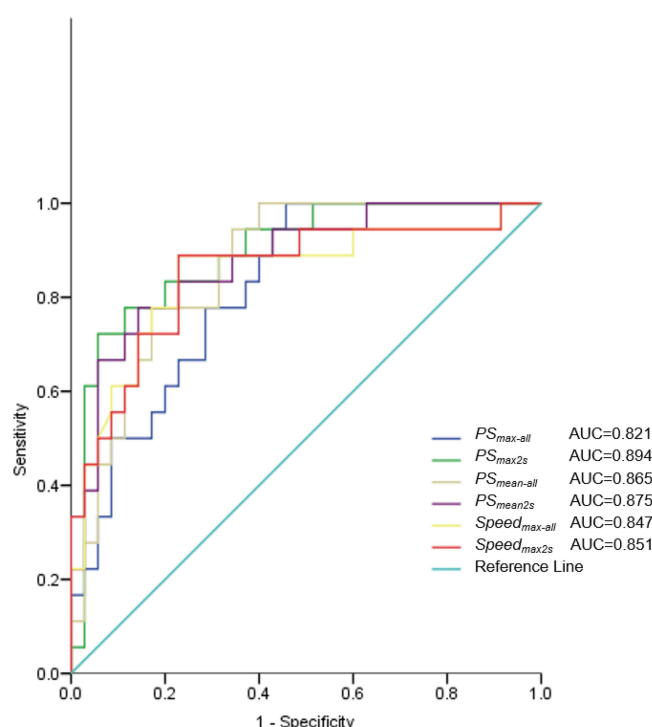| Strain-Related Parameters		Cut-off value	Accuracy	Sensitivity	Specificity
Whole expiration	$PS_{max-all}$	378.76	69.91	54.29	100
	$PS_{mean-all}$	38.46	81.13	82.86	77.78
	$Speed_{max-all}$	27.09	81.13	77.14	88.89
First 2s of expiration	PS_{max2s}	65.48	86.79	94.29	72.22
	PS_{mean2s}	13.18	83.02	85.71	77.78
	$Speed_{max2s}$	23.34	83.02	80.00	88.89

Figure 3 Receiver-operating characteristic curve for strain-related parameters in distinguishing COPD patients from non-COPD ones.

some degree, and it also provides promising imaging biomarkers to assess severity of airflow limitation. Our study added to the growing body of evidence supporting the utility of strain measurement in quantitative analysis of COPD.[17]

Strain measurements is closely related structural changes in lung. Even though COPD has been classified into several phenotype basing on morphologic appearance on CT,[3–6] the extent of structure destruction does not always correlate with the severity of expiratory airflow limitation, which is a set of comprehensive physical phenomenon involving the elastic recoil pressure and the expiratory flow-volume curve.[1,2,4,7,25,26] To complicate matters further, multiple patterns of morphologic changes such as emphysema, bronchial wall thickening, or expiratory air trapping always coexist,[3–6,11] and it is exceedingly difficult to quantify their contributions to airflow limitation separately. Hence, it was no wonder that correlation coefficients were variable between strain-related parameters and different spirometric items.

Theoretically, PS_{max} and PS_{mean} represent the maximum and average degree of deformation in the displacement field, respectively. And $Speed_{max}$ represents the maximum displacement speed in the same field. Thus, lower values of strain-related parameters observed in COPD patients in the present study indicated that either motion extent or speed was decreased during expiration in COPD patients, then reflecting impairment of lung function. Interestingly, emphysematous destruction with decreased values of strain-related parameters was observed in the upper lobes of some non-COPD patients, whereas no abnormalities have been shown yet by spirometry. This phenomenon indirectly confirmed that the extent of structure destruction was not linear correlation with the change of lung function,[7–11,27] meanwhile, identify that strain analysis is sensitive enough to detect the regional functional abnormalities prior to the functional parameters given by spirometry.

In this study, we excluded obvious disorders (eg, respiratory infection, interstitial lung diseases) in pulmonary that could affect quantitative measurement. Actually, GOLD III/IV patients often accompanied with the aforementioned abnormalities. This was also one of the reasons for the limited cases of GOLD III/IV (only 4 cases) in the study population. According to severity of airflow limitation, COPD patients were divided into two subgroups: mild (GOLD I) and moderate to severe (GOLD II–IV) groups, only parameters derived from the whole expiration phase ($PS_{max-all}$, $Speed_{max-all}$) demonstrated statistical difference between the two groups. Even though decreased trend was observed in parameters derived from the first 2s of expiration phase in GOLD II–IV group. This finding may indicate that parameters

of the whole expiration phase may be more sensitive to subtle differences that occur as airflow limitation progresses. However, considering the limited sample size and non-linear correlation between strain measurements and lung function discussed above, further analysis needs to be performed with much larger cohort.

The present study has a number of limitations. First, a limited number of patients were enrolled, and considering the burden of second-hand smoke exposure among non-smokers in China,[28] those subjects with long-term passive smoke exposure were also enrolled, which was different from the inclusion criteria used in other COPD-related studies,[5,17] thus our study results need to be verified in further study. Second, COPD patients with severe airflow limitation (GOLD III–IV) were underrepresented and aggregated with GOLD II patients into a single group for analysis, so our results cannot be generalized to more severe COPD population. Third, since the airflow obstruction of COPD is more severe in expiration phase during ventilation, we focused on strain analysis for the expiration phase only in this study. Fourth, various breathing patterns (eg, chest breathing, abdominal breathing) in patients were not assessed, which may have influenced the final results.[18] Fifth, due to limited scan length in the Z-axis (Z_{max}=16cm), currently, a whole-lung dynamic-ventilation CT scan needs two volume scans to complete. Even though a low-dose CT scan protocol combined with an advanced iterative reconstruction method (AIDR3D) was adopted,[29] increased radiation exposure was unavoidable. In the further study, AiCE (advanced intelligent clear-IQ engine) technology, which is a novel reconstruction method involving deep learning and AI technologies,[30,31] would be actively conducted to reduce radiation dose as far as possible. In addition, since data from two CT volume packages needed to match and joint together for pro-processing, even though the motion coherence algorithm can be selected, subject cooperation was quite important to acquire high-quality images. In this study, 11 subjects have been excluded for poor cooperation with voice guidance during CT scans.

In conclusion, strain-related parameters derived from dynamic-ventilation CT data covering the whole lung associated with lung function changes in COPD, reflecting the severity of airflow limitation in some degree, even though its utility in severe COPD patients remains to be investigated. Our results would also be an evidence for the feasibility of monitoring lung function using strain analysis in the future.

Funding

Disclosure

Yanyan Xu received a research grant from China-Japan Friendship Hospital (2019-1-QN-60). The authors report no other conflicts of interest in this work.

References

1. Celli BR, Wedzicha JA. Update on clinical aspects of chronic obstructive pulmonary disease. *N Engl J Med*. 2019;381(13):1257–1266. doi:10.1056/NEJMra1900500
2. Celli BR, MacNee W; ATS/ERS Task Force. Standards for the diagnosis and treatment of patients with COPD: a summary of the ATS/ERS position paper. *Eur Respir J*. 2006;27(1):242.
3. Matsuoka S, Yamashiro T, Washko GR, Kurihara Y, Nakajima Y, Hatabu H. Quantitative CT assessment of chronic obstructive pulmonary disease. *Radiographics*. 2010;30(1):55–66. doi:10.1148/rg.301095110
4. Kang HS, Bak SH, Oh HY, et al. Computed tomography-based visual assessment of chronic obstructive pulmonary disease: comparison with pulmonary function test and quantitative computed tomography. *J Thorac Dis*. 2021;13(3):1495–1506. doi:10.21037/jtd-20-3041
5. MacNeil JL, Capaldi DPI, Westcott AR, et al. Pulmonary imaging phenotypes of chronic obstructive pulmonary disease using multiparametric response maps. *Radiology*. 2020;295(1):227–236. doi:10.1148/radiol.2020191735
6. Park J, Hobbs BD, Crapo JD, et al. Subtyping COPD by using visual and quantitative CT imaging features. *Chest*. 2020;157(1):47–60. doi:10.1016/j.chest.2019.06.015
7. Feldhaus FW, Theilig DC, Hubner RH, Kuhnigk JM, Neumann K, Doellinger F. Quantitative CT analysis in patients with pulmonary emphysema: is lung function influenced by concomitant unspecific pulmonary fibrosis? *Int J Chron Obstruct Pulmon Dis*. 2019;14:1583–1593. doi:10.2147/COPD.S204007
8. Oh AS, Strand M, Pratte K, et al. Visual emphysema at chest CT in GOLD Stage 0 cigarette smokers predicts disease progression: results from the COPDGene study. *Radiology*. 2020;296(3):641–649. doi:10.1148/radiol.2020192429
9. Cosío BG, Pascual-Guardia S, Borras-Santos A, et al. Phenotypic characterisation of early COPD: a prospective case-control study. *ERJ Open Res*. 2020;6(4):00047–2020. doi:10.1183/23120541.00047-2020
10. El Kaddouri B, Strand MJ, Baraghoshi D, et al. Fleischner society visual emphysema CT patterns help predict progression of emphysema in current and former smokers: results from the COPDGene study. *Radiology*. 2021;298(2):441–449. doi:10.1148/radiol.2020200563

11. Virdee S, Tan WC, Hogg JC, et al. Spatial dependence of CT emphysema in chronic obstructive pulmonary disease quantified by using join-count statistics. *Radiology*. 2021;301(3):702–709. doi:10.1148/radiol.2021210198

12. Lange P, Halpin DM, O'Donnell DE, MacNee W. Diagnosis, assessment, and phenotyping of COPD: beyond FEV₁. *Int J Chron Obstruct Pulmon Dis*. 2016;11:3–12.

13. Regan EA, Hokanson JE, Murphy JR, et al. Genetic epidemiology of COPD (COPDGene) study design. *COPD*. 2010;7(1):32–43. doi:10.3109/15412550903499522

14. Couper D, LaVange LM, Han M, et al.; SPIROMICS Research Group. Design of the subpopulations and intermediate outcomes in COPD study (SPIROMICS). *Thorax*. 2014;69(5):491–494. doi:10.1136/thoraxjnl-2013-203897.

15. Thomashow MA, Shimbo D, Parikh MA, et al. Endothelial microparticles in mild chronic obstructive pulmonary disease and emphysema. The multi-ethnic study of atherosclerosis chronic obstructive pulmonary disease study. *Am J Respir Crit Care Med*. 2013;188(1):60–68. doi:10.1164/rccm.201209-1697OC

16. Yamashiro T, Moriya H, Matsuoka S, et al. Asynchrony in respiratory movements between the pulmonary lobes in patients with COPD: continuous measurement of lung density by 4-dimensional dynamic-ventilation CT. *Int J Chron Obstruct Pulmon Dis*. 2017;12:2101–2109. doi:10.2147/COPD.S140247

17. Xu Y, Yamashiro T, Moriya H, et al. Strain measurement on four-dimensional dynamic-ventilation CT: quantitative analysis of abnormal respiratory deformation of the lung in COPD. *Int J Chron Obstruct Pulmon Dis*. 2018;14:65–72. doi:10.2147/COPD.S183740

18. Mochizuki E, Kawai Y, Morikawa K, et al. Difference in local lung movement during tidal breathing between COPD patients and asthma patients assessed by four-dimensional dynamic-ventilation CT scan. *Int J Chron Obstruct Pulmon Dis*. 2020;15:3013–3023. doi:10.2147/COPD.S273425

19. Cruces P, Erranz B, Lillo F, et al. Mapping regional strain in anesthetised healthy subjects during spontaneous ventilation. *BMJ Open Respir Res*. 2019;6(1):e000423. doi:10.1136/bmjresp-2019-000423

20. Tanabe Y, Kido T, Kurata A, et al. Three-dimensional maximum principal strain using cardiac computed tomography for identification of myocardial infarction. *Eur Radiol*. 2017;27(4):1667–1675. doi:10.1007/s00330-016-4550-9

21. Joseph S, Moazami N, Cupps BP, et al. Magnetic resonance imaging-based multiparametric systolic strain analysis and regional contractile heterogeneity in patients with dilated cardiomyopathy. *J Heart Lung Transplant*. 2009;28(4):388–394. doi:10.1016/j.healun.2008.12.018

22. Haugaa KH, Smedsrud MK, Steen T, et al. Mechanical dispersion assessed by myocardial strain in patients after myocardial infarction for risk prediction of ventricular arrhythmia. *JACC Cardiovasc Imaging*. 2010;3(3):247–256. doi:10.1016/j.jcmg.2009.11.012

23. Niu J, Zeng M, Wang Y, et al. Sensitive marker for evaluation of hypertensive heart disease: extracellular volume and myocardial strain. *BMC Cardiovasc Disord*. 2020;20(1):292. doi:10.1186/s12872-020-01553-7

24. Huda W, Ogden KM, Khorasani MR. Converting dose-length product to effective dose at CT. *Radiology*. 2008;248(3):995–1003. doi:10.1148/radiol.2483071964

25. Jacob J, Bartholmai BJ, Rajagopalan S, et al. Serial automated quantitative CT analysis in idiopathic pulmonary fibrosis: functional correlations and comparison with changes in visual CT scores. *Eur Radiol*. 2018;28(3):1318–1327. doi:10.1007/s00330-017-5053-z

26. Bates JH. Systems physiology of the airways in health and obstructive pulmonary disease. *Wiley Interdiscip Rev Syst Biol Med*. 2016;8(5):423–437. doi:10.1002/wsbm.1347

27. Bodduluri S, Bhatt SP, Hoffman EA, et al.; COPDGene Investigators. Biomechanical CT metrics are associated with patient outcomes in COPD. *Thorax*. 2017;72(5):409–414. doi:10.1136/thoraxjnl-2016-209544

28. Xiao L, Jiang Y, Zhang J, Parascandola M. Secondhand smoke exposure among nonsmokers in China. *Asian Pac J Cancer Prev*. 2020;21(S1):17–22. doi:10.31557/APJCP.2020.21.1.1

29. Yamashiro T, Miyara T, Honda O, et al. Iterative reconstruction for quantitative computed tomography analysis of emphysema: consistent results using different tube currents. *Int J Chron Obstruct Pulmon Dis*. 2015;10:321–327. doi:10.2147/COPD.S74810

30. Nakamura Y, Higaki T, Tatsugami F, et al. possibility of deep learning in medical imaging focusing improvement of computed tomography image quality. *J Comput Assist Tomogr*. 2020;44(2):161–167. doi:10.1097/RCT.0000000000000928

31. Singh R, Digumarthy SR, Muse VV, et al. Image quality and lesion detection on deep learning reconstruction and iterative reconstruction of submillisievert chest and abdominal CT. *AJR Am J Roentgenol*. 2020;214(3):566–573. doi:10.2214/AJR.19.21809